Bicarbonate transport in sheep parotid secretory cells

M. C. Steward*, P. Poronnik and D. I. Cook

Department of Physiology, University of Sydney, Sydney, NSW 2006, Australia

1. Intracellular pH (pH_i) was measured by microfluorimetry in secretory endpieces isolated from sheep parotid glands and loaded with the pH-sensitive fluoroprobe 2′,7′-bis(2-carboxyethyl)-5(6)-carboxyfluorescein (BCECF).

2. Stimulation with 1 μM acetylcholine (ACh) caused a large, transient decrease in pH_i of 0·37 ± 0·02 pH units followed by a slower recovery. The transient, which was reduced by 60% in the absence of HCO_3^-, could be attributed mainly to HCO_3^- efflux. During sustained stimulation, pH_i increased to a value that exceeded the resting value by 0·083 ± 0·023 pH units after 20 min.

3. The anion channel blocker NPPB (0·1 mM) reduced the transient acidification in response to ACh by 48% and raised pH_i during sustained stimulation. Simultaneous application of NPPB and ACh accelerated the re-alkalinization following the initial acidification, indicating that NPPB inhibits HCO_3^- efflux.

4. The stilbene derivative H_2DIDS (0·5 mM) reduced the transient acidification in response to ACh by 76% but caused a marked decrease in pH_i during sustained stimulation. Simultaneous application of H_2DIDS and ACh slowed the re-alkalinization following the initial acidification, indicating that the main effect of H_2DIDS was to inhibit HCO_3^- accumulation.

5. In the absence of HCO_3^-, the recovery from an acid load was unaffected by ACh stimulation. Acid extrusion, although dependent on Na^+, was not inhibited by amiloride (1 mM), clonidine (1 mM) or H_2DIDS (0·5 mM) and was therefore provisionally attributed to a Na^+–H^+ exchanger isoform other than NHE1 or NHE2.

6. In the presence of HCO_3^-, the rate of recovery from an acid load was reduced during ACh stimulation, probably as a result of the increased efflux of HCO_3^-. Acid extrusion was dependent on Na^+ and was significantly inhibited by H_2DIDS.

7. We conclude that ACh-evoked HCO_3^- secretion in the sheep parotid gland differs from that in many other salivary glands by being driven predominantly by basolateral Na^+–HCO_3^- cotransport rather than by Na^+–H^+ exchange.

The parotid glands of ruminants and other foregut fermenters, such as camels and kangaroos, differ from other mammalian salivary glands in secreting a HCO_3^--rich saliva (Hoppe, Kay & Maloiy, 1975; Young & Van Lennep, 1979; Beal, 1984; Cook, 1995). The relationship between the electrolyte concentrations and the salivary flow rate suggests that in these glands the primary secretion itself contains a high concentration of HCO_3^- and that the ductal contribution is small. In the salivary glands of most common laboratory species, the primary secretion is Cl^- rich and is driven by the secondary active transport of Cl^- across the basolateral membrane of the secretory cells (reviewed by Cook, Van Lennep, Roberts & Young, 1994). In contrast, the Cl^- concentration in the primary fluid of the sheep parotid is only about 50 mM (Compton, Nelson, Wright & Young, 1980), and furosemide (frusemide), which blocks the accumulation of intracellular Cl^-, has little effect on saliva flow *in vivo* (Wright, Blair-West & Nelson, 1986). Furthermore, in the bovine parotid, $^{86}Rb^+$ efflux data suggest that salivary secretion is driven almost exclusively by HCO_3^- transport (Lee & Turner, 1992).

Evidently, the mechanism responsible for the primary secretion in ruminant parotid glands is different from that in glands that generate a Cl^--rich primary fluid. In some respects, it may more closely resemble the secretin-stimulated pancreatic duct. Thus, by analogy with the pancreas (reviewed by Case & Argent, 1993), intracellular HCO_3^- might be generated from CO_2 through the action of

* To whom correspondence should be addressed at the School of Biological Sciences, G.38 Stopford Building, University of Manchester, Manchester M13 9PT, UK.

carbonic anhydrase combined with the extrusion of protons across the basolateral membrane via a Na^+–H^+ exchanger or a H^+-ATPase. Alternatively, HCO_3^- itself might be taken up across the basolateral membrane. The principal aim of the present study was therefore to characterize the transporters responsible for HCO_3^- accumulation in the parotid gland of the sheep.

The sheep parotid produces a saliva containing 110–140 mM HCO_3^- over a wide range of secretory rates (Coats & Wright, 1957). It has already been shown to express an amiloride-insensitive isoform of the Na^+–H^+ exchanger (Poronnik, Young & Cook, 1993). This may explain why amiloride has little effect on fluid secretion *in vivo* (Wright *et al.* 1986), but it does not necessarily indicate that Na^+–H^+ exchange provides the main driving force for HCO_3^- accumulation. Indeed, other *in vivo* studies have shown that carbonic anhydrase inhibitors only reduce the saliva flow and HCO_3^- output by about 40% (Blair-West, Fernley, Nelson, Wintour & Wright, 1980) suggesting that CO_2 is not the only source of intracellular HCO_3^-.

Our recent studies of the HCO_3^- dependence of intracellular Na^+ concentration and cell volume indicate that a Na^+–HCO_3^- cotransporter may be involved in the uptake of HCO_3^- from the interstitium (Poronnik, Schumann & Cook, 1995). To test this hypothesis, we have investigated HCO_3^- transport in the sheep parotid by measuring intracellular pH (pH_i) in isolated secretory endpieces loaded with the pH-sensitive fluoroprobe 2′,7′-bis(2-carboxyethyl)-5(6)-carboxyfluorescein (BCECF). The effects of anion transport inhibitors were examined on unstimulated cells, on the initial transient response to muscarinic stimulation, and during sustained stimulation. Since we were unable to inhibit the Na^+–H^+ exchanger, the contribution of HCO_3^- uptake to the recovery of pH_i following acid loading was investigated by comparing the recovery rates in the presence and absence of HCO_3^- and their sensitivity to stilbenes. The principal finding is that, during sustained secretion, a significant fraction of the HCO_3^- flux is driven by Na^+-dependent, stilbene-sensitive HCO_3^- uptake, most probably via a Na^+–HCO_3^- cotransporter.

METHODS

Preparation of parotid gland secretory endpieces

Cross-bred Merino sheep, fed on a mixture of lucerne and oaten chaff (30%:70%) with water *ad libitum*, were killed with a captive-bolt pistol. The parotid glands were excised rapidly and placed on ice. Small pieces of gland, trimmed of fat and connective tissue, were chopped finely and incubated in a Hepes-buffered solution containing collagenase (50–75 U ml^{-1}, Type IV, Worthington) for 15–25 min at 37 °C in a shaking water bath. The fragments were then sieved though a 200 μm nylon mesh and subjected to gentle trituration with a syringe. The suspension was then washed three times and resuspended in a small volume of the Hepes solution. The endpieces were loaded with the pH-sensitive fluoroprobe 2′,7′-bis(2-carboxyethyl)-5(6)-carboxyfluorescein (BCECF) by adding the acetoxymethyl ester (BCECF-AM, Molecular Probes) at a concentration of 2·5 μM and incubating for 15 min at room temperature. The endpieces were then washed twice, resuspended in the Hepes solution and stored on ice until required.

Prior to use, a small volume of the suspension was pipetted on to a coverslip which formed the base of a slot-shaped Perspex chamber. The endpieces were allowed to settle and attach to the glass. A second coverslip was sealed on to the top of the chamber which was then perfused at 1 ml min^{-1}. Solutions were gassed at 37 °C and the temperature of the perfusion solution in the tubing was maintained by a heated water jacket. The pH of the solution was monitored with a micro-combination needle electrode (type 812, Diamond General, Ann Arbor, MI, USA) inserted into the perfusion line close to the chamber, and the temperature of the chamber was monitored with a bead thermistor.

Microfluorimetry

Fluorescence was measured at 530 nm using a Nikon Diaphot inverted microscope equipped with epifluorescence and a × 40 Fluor objective lens. Single BCECF-loaded endpieces consisting of between ten and twenty cells were illuminated alternately at 430 and 490 nm. Fluorescence intensity was sampled for 100 ms at each wavelength using a MacLab-4 data acquisition system (AD Instruments, Sydney, Australia) and the cycle was repeated at 5 s intervals. Calibration of the fluorescence ratio F_{490}/F_{430} was performed by the nigericin–high-K^+ method (Thomas, Buchsbaum, Zimniak & Racker, 1979). The relationship between F_{490}/F_{430} and pH_i was found to be linear over a pH range from 6·6 to 7·8 and was highly reproducible. Calibration was, therefore, only checked occasionally and the perfusion line subsequently washed thoroughly. Data are plotted in some of the figures as means (continuous lines) ± S.E.M. (dotted lines).

Buffering capacity and acid–base fluxes

Intrinsic buffering capacity (β_i) was measured as a function of pH_i in nominally HCO_3^--free conditions according to the method of Weintraub and Machen (1989). The endpieces were exposed first for 10 min to the Na^+-free Hepes solution. This resulted in a decrease in pH_i and it abolished any Na^+-dependent pH regulatory mechanisms. The cells were then stepped through a series of solutions containing decreasing concentrations of NH_4Cl (20, 10, 5, and 0 mM). The changes in pH_i (ΔpH_i) caused by the step changes in $[NH_4^+]_o$, and the corresponding changes in intracellular NH_4^+ concentration $\Delta[NH_4^+]_i$ (calculated from pH_i assuming the −log of the acid dissociation constant (pK_a) = 8·9) were used to estimate the value of β_i at the mid-point of each pH interval:

$$\beta_i = \Delta[NH_4^+]_i/\Delta pH_i.$$

Further measurements were obtained using trimethylamine (pK_a = 9·4) in place of NH_4^+ (Szatkowski & Thomas, 1989). The pooled data were plotted as a function of pH_i and fitted by a sigmoid curve. The expected total buffering capacity (β_t) in HCO_3^--buffered solutions was calculated as a function of pH_i using (Weintraub & Machen, 1989):

$$\beta_t = \beta_i + 2{\cdot}3\,[HCO_3^-]_i.$$

Acid–base fluxes were calculated from the pH_i changes that accompanied the withdrawal or restoration of extracellular Na^+ by first curve-fitting the data with a 4th-order polynomial. The rate of change of pH_i obtained from the first derivative of this function was then multiplied by β_i or β_t as appropriate to give a net acid–base flux in millimoles per litre per minute. A positive flux indicates proton extrusion or HCO_3^- uptake. Data are presented as the means ± S.E.M., and statistical comparisons have been made using Student's unpaired *t* test.

Solutions and materials

The Hepes-buffered solution used for endpiece preparation and as the control solution for nominally HCO_3^--free experiments contained (mM): NaCl, 140; KCl, 5; $CaCl_2$, 1; $MgCl_2$, 1; Hepes, 4·4; Na-Hepes, 5·6; D-glucose, 5. The pH was 7·4 at 37 °C and the solution was gassed continuously with 100% O_2. The HCO_3^--buffered solution contained (mM): NaCl, 120; $NaHCO_3$, 25; KCl, 5; $CaCl_2$, 1; $MgCl_2$, 1; Hepes, 2·2; Na-Hepes, 2·8; D-glucose, 5; and was gassed at 37 °C with 5% CO_2–95% O_2. Na^+-free solutions were prepared by equimolar substitution of *N*-methyl-D-glucamine ($NMDG^+$) for Na^+. NMDG-HCO_3 was prepared by gassing a 1 M solution of NMDG overnight with 100% CO_2. In the Cl^--free solutions, gluconate replaced most of the Cl^-, and $CaCl_2$ and $MgCl_2$ were replaced by $CaSO_4$ and $MgSO_4$, respectively. The concentration of $CaSO_4$ was increased to 2 mM to compensate for the binding of Ca^{2+} to gluconate. NH_4Cl was added to solutions by equimolar substitution for NaCl. The high-K^+ pH calibration solution contained (mM): NaCl, 10; KCl, 130; $CaCl_2$, 1; $MgCl_2$, 1; Hepes, 20. Nigericin was added to this from a 5 mM stock solution in ethanol to give a final concentration of 5 μM, and the pH was adjusted at 37 °C to four values in the range from 6·6 to 7·8.

Acetylcholine chloride (ACh), amiloride hydrochloride, clonidine hydrochloride, *N*-methyl-D-glucamine (NMDG), nigericin and trimethylamine hydrochloride were obtained from Sigma. 4,4′-Diisothiocyanatodihydrostilbene-2,2′-disulphonic acid (H_2DIDS) was obtained from Molecular Probes. 5-Nitro-2-(3-phenylpropylamino)-benzoate (NPPB) was a gift from Professor R. Greger (University of Freiburg, Germany). All other chemicals were of at least analytical reagent grade.

RESULTS

The average value of pH_i in unstimulated parotid endpieces superfused with a nominally HCO_3^--free, Hepes-buffered solution was 7·36 ± 0·02 (mean ± S.E.M., $n = 18$). In the presence of HCO_3^-, pH_i was 7·19 ± 0·02 ($n = 57$). The response to stimulation with 1 μM ACh, which evokes maximal fluid secretion in perfused glands from other species, consisted of a transient decrease in pH_i (Fig. 1*A*). The average decrease measured in fifty-one endpieces in the presence of HCO_3^- was −0·37 ± 0·02 pH units. This is larger than the transient reported in the rat parotid (Nauntofte & Dissing, 1988) and in the rabbit mandibular gland (Lau, Elliott & Brown, 1989; Steward, Seo & Case, 1989). After the initial decrease, pH_i recovered towards its resting value. In six experiments in which stimulation with ACh was maintained for 20 min, pH_i recovered to its resting level after about 5 min and then continued to increase slowly. At the end of the 20 min period, pH_i exceeded the initial control value by 0·083 ± 0·023 pH units ($P < 0·05$).

In glands from other species, the transient decrease in pH_i evoked by muscarinic stimulation has been attributed to HCO_3^- efflux across the luminal membrane (Melvin, Moran & Turner, 1988; Nauntofte & Dissing, 1988; Lau *et al.* 1989; Steward *et al.* 1989). In the sheep parotid endpieces, omission of HCO_3^- from the superfusate (Fig. 1*B*) resulted in a significantly smaller decrease in pH_i (−0·148 ± 0·013 pH units, $n = 23$, $P < 0·001$). Although the response was not entirely abolished, it is clear that a significant part can be attributed to HCO_3^- efflux. The small acidification that remained may have been due to the efflux of HCO_3^- derived from residual metabolic CO_2 or to the increased production of metabolic acid.

Inhibitors of anion transport

The Cl^- channel blocker NPPB (0·1 mM) had little effect on resting pH_i but the response to 1 μM ACh in the presence of HCO_3^- was attenuated (Fig. 2*A*). The change in pH_i upon

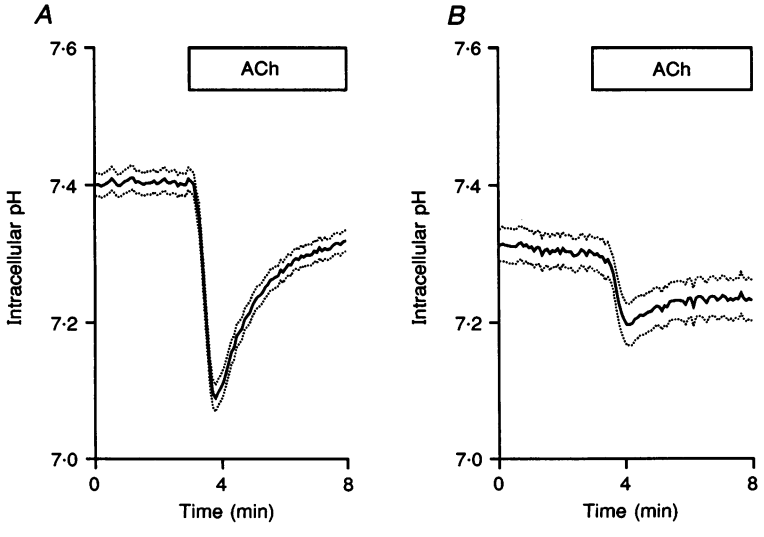

Figure 1. Changes in intracellular pH following stimulation with ACh

Initial effects of 1 μM ACh on pH_i in sheep parotid endpieces in a HCO_3^--buffered solution containing 25 mM HCO_3^- ($n = 51$) (*A*) and in a nominally HCO_3^--free, Hepes-buffered solution ($n = 23$) (*B*). Open bars indicate period of application. Data in this, and other figures, are plotted as means (continuous lines) ± S.E.M. (dotted lines).

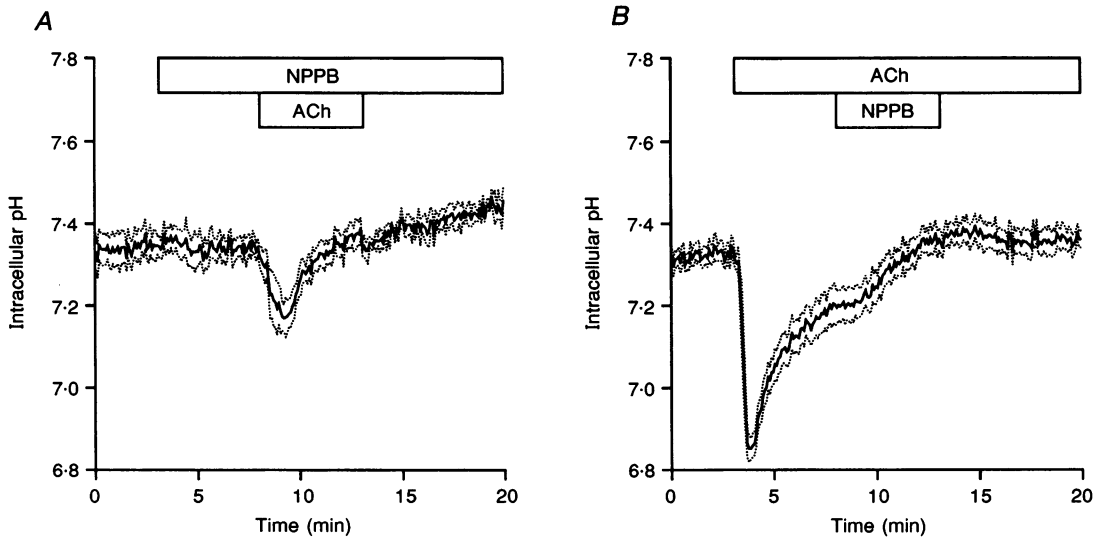

Figure 2. Inhibition of HCO_3^- efflux by NPPB

Effects of 0·1 mM NPPB on the initial response to 1 μM ACh ($n = 5$) (*A*) and when applied during sustained stimulation with ACh ($n = 5$) (*B*). The superfusate contained 25 mM HCO_3^-.

stimulation was $-0{\cdot}235 \pm 0{\cdot}044$ pH units ($n = 5$). This compares with a control response, in endpieces from the same glands (Fig. 2*B*), of $-0{\cdot}455 \pm 0{\cdot}027$ pH units ($n = 8$, $P < 0{\cdot}01$). It suggests that HCO_3^- either leaves the cells through an NPPB-sensitive non-selective anion channel, as proposed in the rabbit mandibular gland (Brown, Elliott & Lau, 1989) and rat parotid (Melvin *et al.* 1988; Lee & Turner, 1991), or by Cl^-–HCO_3^- exchange in parallel with an NPPB-sensitive Cl^- channel, as in the rat pancreatic duct (Gray, Greenwell & Argent, 1988; Novak & Greger, 1988). The latter possibility can be excluded since replacement of the bath Cl^- by gluconate did not reduce the magnitude of the transient acidification: the change in pH_i in response to ACh was $-0{\cdot}368 \pm 0{\cdot}038$ pH units ($n = 11$) compared with $-0{\cdot}326 \pm 0{\cdot}036$ pH units ($n = 12$) in the corresponding control experiments. Nor did Cl^- replacement affect the rate of re-alkalinization: the initial rate of recovery of pH_i was $0{\cdot}113 \pm 0{\cdot}019$ pH units min^{-1} in the absence of Cl^- compared with $0{\cdot}121 \pm 0{\cdot}019$ pH units min^{-1} in the control experiments.

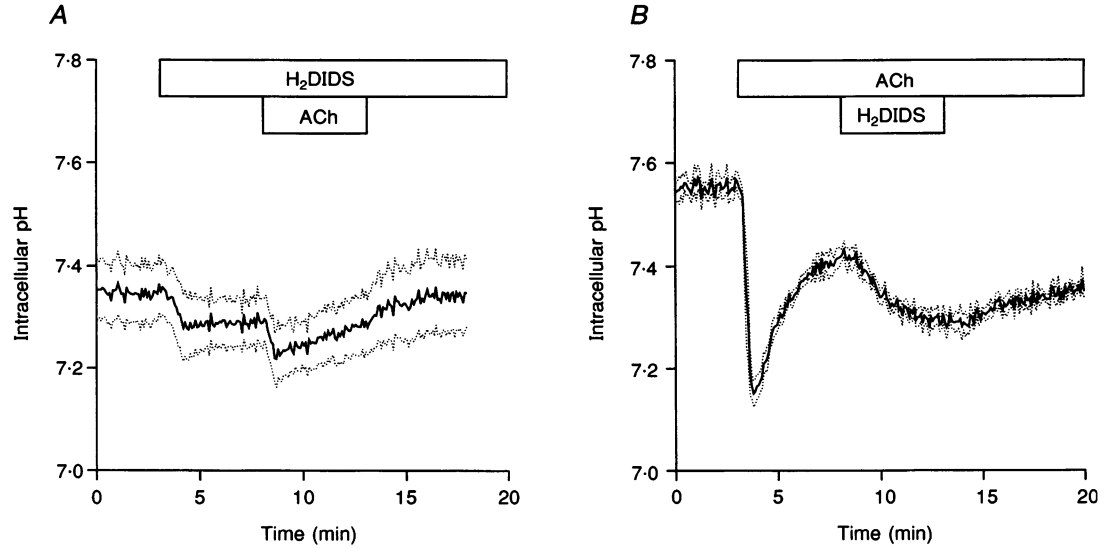

Figure 3. Inhibition of HCO_3^- uptake by H_2DIDS

Effects of 0·5 mM H_2DIDS on the initial response to 1 μM ACh ($n = 7$) (*A*) and when applied during sustained stimulation with ACh ($n = 5$) (*B*). The superfusate contained 25 mM HCO_3^-.

When NPPB was applied during sustained ACh stimulation (Fig. 2*B*), the rate of increase in pH_i was accelerated from $0{\cdot}018 \pm 0{\cdot}004$ to $0{\cdot}053 \pm 0{\cdot}008$ pH units min^{-1} ($n = 5$, $P < 0{\cdot}05$). Furthermore, pH_i increased to a steady-state value that was significantly higher than in the corresponding control response to ACh. This is consistent with NPPB blocking HCO_3^- efflux, and with the throughput of HCO_3^- being greater during ACh stimulation than at rest.

Another blocker of anion transport, the stilbene derivative H_2DIDS (Lepke, Fasold, Pring & Passow, 1976), had quite a different effect. When applied to unstimulated endpieces (Fig. 3*A*), 0·5 mM H_2DIDS caused a small decrease in pH_i suggesting that, in the resting state, it might have an inhibitory effect on HCO_3^- uptake. When the endpieces were then stimulated with 1 μM ACh in the presence of H_2DIDS, the transient decrease in pH_i was reduced to $-0{\cdot}106 \pm 0{\cdot}023$ pH units ($n = 7$, $P < 0{\cdot}001$) compared with the corresponding control response to ACh (data not shown) of $-0{\cdot}310 \pm 0{\cdot}020$ pH units ($n = 6$). Although the initial decrease in pH_i, caused by H_2DIDS, reduced the driving force for HCO_3^- efflux, the value to which pH_i dropped following ACh stimulation ($7{\cdot}183 \pm 0{\cdot}049$) was not as low as in the control experiments ($6{\cdot}981 \pm 0{\cdot}053$, $P < 0{\cdot}05$). It is therefore possible that H_2DIDS, like NPPB, has an inhibitory effect on HCO_3^- efflux.

However, in contrast to NPPB, application of H_2DIDS during ACh stimulation (Fig. 3*B*) caused a large *decrease* in pH_i. If the effect of H_2DIDS had been only to block HCO_3^- efflux, pH_i would have increased as it did with NPPB. The fact that it decreased markedly suggests that the more significant effect of H_2DIDS was to reduce HCO_3^- uptake.

Further support for this interpretation was obtained when the inhibitors were applied simultaneously with ACh (Fig. 4). The advantage of this protocol was that the effect of the inhibitors on HCO_3^- uptake and efflux only became manifest after the initial acidification had occurred.

In eight control experiments (Fig. 4*A*), ACh stimulation caused a transient acidification of $-0{\cdot}278 \pm 0{\cdot}034$ pH units and the initial rate of recovery was $0{\cdot}114 \pm 0{\cdot}017$ pH units min^{-1}. When H_2DIDS was applied simultaneously with ACh (Fig. 4*B*), the transient acidification ($-0{\cdot}246 \pm 0{\cdot}057$ pH units, $n = 5$) was undiminished, but the initial rate of recovery was reduced by 66% to $0{\cdot}039 \pm 0{\cdot}010$ pH units min^{-1}. NPPB applied simultaneously with ACh (Fig. 4*C*) also had no significant effect on the transient acidification ($-0{\cdot}251 \pm 0{\cdot}038$ pH units, $n = 6$) but it increased the rate of recovery by 50% to $0{\cdot}171 \pm 0{\cdot}019$ pH units min^{-1}.

The most plausible interpretation of these data is that H_2DIDS slowed the recovery by blocking HCO_3^- uptake whereas NPPB accelerated the recovery by blocking HCO_3^- efflux. When both inhibitors were applied simultaneously with ACh (data not shown) the two effects cancelled each other out and the recovery rate ($0{\cdot}131 \pm 0{\cdot}020$ pH units min^{-1}, $n = 4$) was not significantly different from the controls.

These results support our hypothesis that the principal effect of H_2DIDS is to inhibit HCO_3^- uptake. Furthermore, it leads to the conclusion that, during stimulation with ACh, a significant fraction of the driving force for HCO_3^- efflux is provided by stilbene-sensitive HCO_3^- uptake rather than by H^+ extrusion via the Na^+–H^+ exchanger.

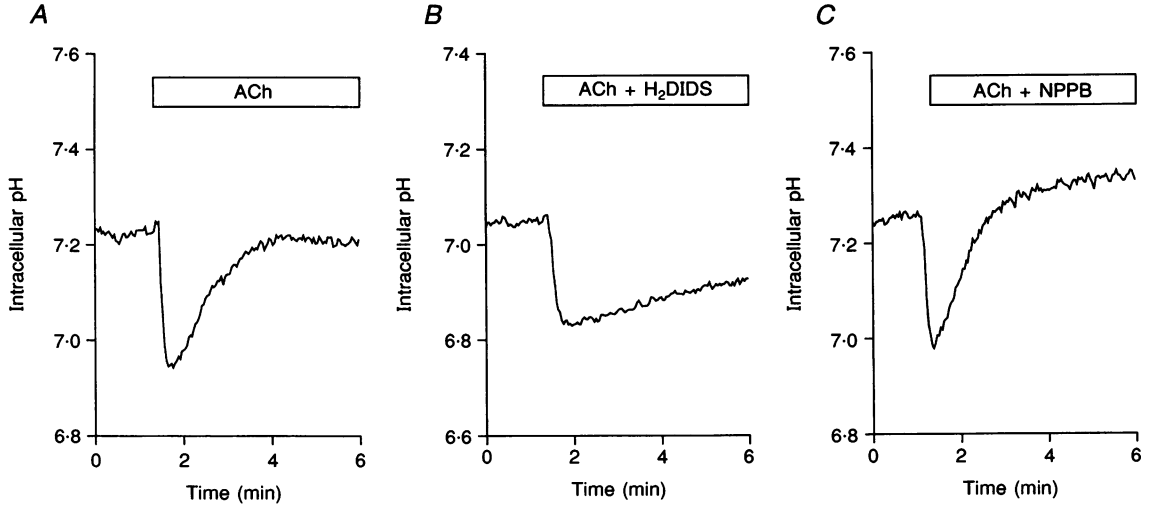

Figure 4. Simultaneous application of ACh and NPPB or H_2DIDS

A, control response to 1 μM ACh in the presence of 25 mM HCO_3^- (1 of 8 experiments). *B*, simultaneous application of 1 μM ACh and 0·5 mM H_2DIDS (1 of 5 experiments). *C*, simultaneous application of 1 μM ACh and 0·1 mM NPPB (1 of 6 experiments).

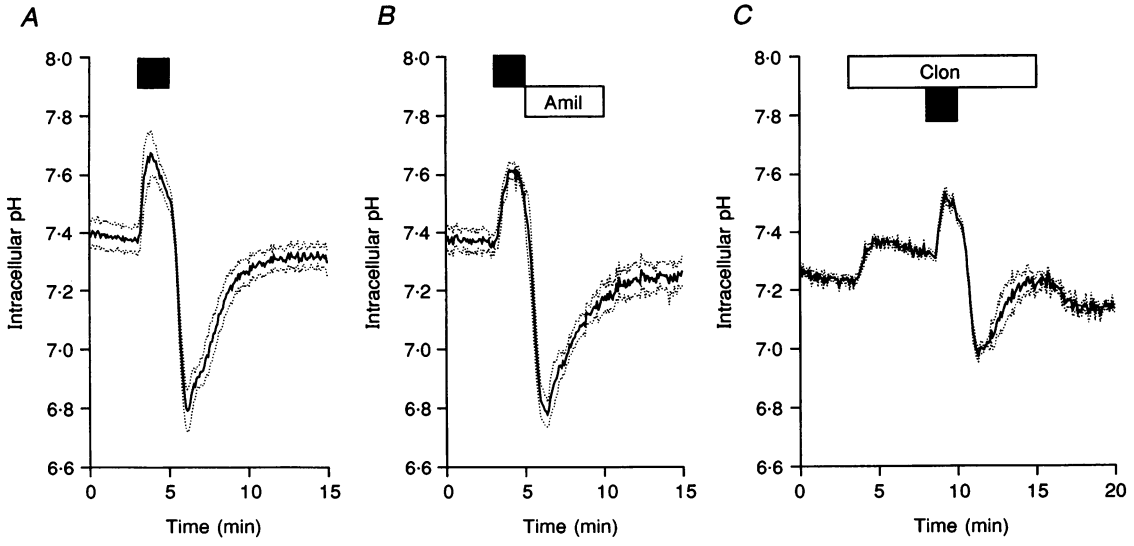

Figure 5. Effects of Na^+–H^+ exchange inhibitors

A, recovery of pH_i following acid loading with a 2 min pulse of 20 mM NH_4Cl (filled bar, $n = 6$). *B*, effect of 1 mM amiloride (Amil) on the recovery of pH_i ($n = 4$). *C*, effect of 1 mM clonidine (Clon) on the recovery of pH_i ($n = 3$). All solutions were nominally HCO_3^- free.

Inhibitors of Na^+–H^+ exchange

Previous work from this laboratory has demonstrated the existence of a Na^+–H^+ exchanger in the sheep parotid that is insensitive to amiloride and its more specific analogues (Poronnik *et al.* 1993). Figure 5 shows the recovery of pH_i in endpiece cells acid loaded by exposure to a 2 min pulse of 20 mM NH_4Cl in the absence of HCO_3^-. When the NH_4Cl pulse was followed by a 5 min exposure to 1 mM amiloride, the rate of recovery was only slightly reduced (Fig. 5*B*) compared with the corresponding controls (Fig. 5*A*).

In a further attempt to characterize this transporter, we examined the effects of the α_2-adrenoceptor agonist clonidine which is known to inhibit the amiloride-insensitive NHE2 isoform of the exchanger (Kulanthaivel *et*

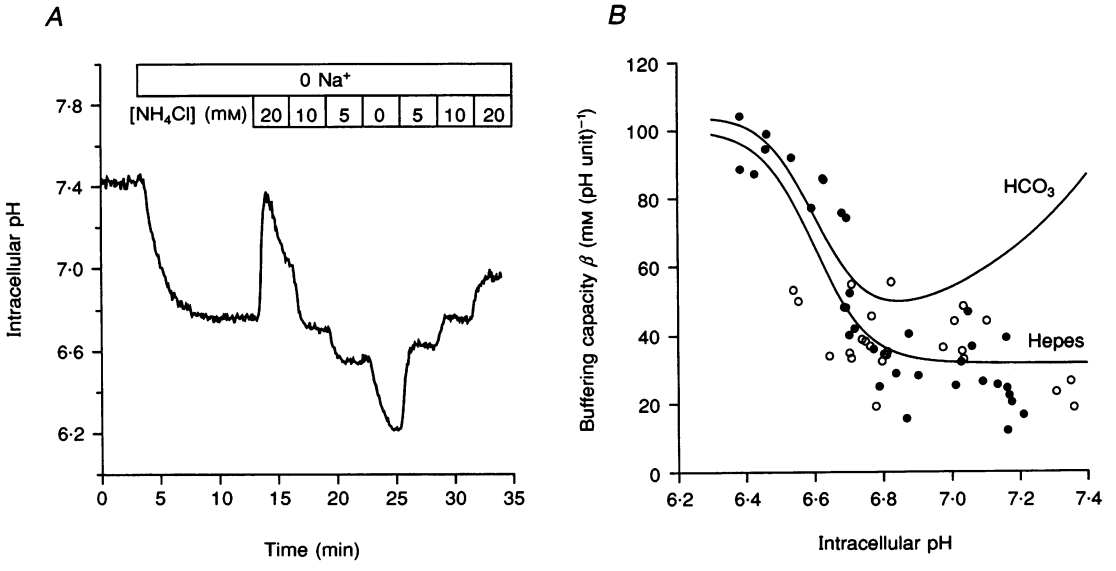

Figure 6. Measurement of intrinsic buffering capacity (β_i)

A, following replacement of extracellular Na^+ with $NMDG^+$, the cells were exposed to a series of NH_4Cl concentrations. Hepes-buffered superfusate. One of 12 experiments. *B*, pooled measurements of β_i obtained with NH_4Cl (●) and trimethylamine (○). Data are fitted by a sigmoid curve (Hepes). The other curve (HCO_3) shows β_t in the presence of 25 mM HCO_3^- (see Methods).

al. 1992). Pretreatment with 1 mM clonidine (Fig. 5*C*) itself caused an increase in pH_i. It also reduced the magnitude of the acidification following the subsequent NH_4Cl pulse. The initial effect of clonidine was probably due to its adrenergic activity since it was largely abolished by the α_2-antagonist yohimbine (10 μM; data not shown) and it may be attributed to an upregulation of the Na^+–H^+ exchanger as has been observed in the rabbit proximal tubule (Nord, Howard, Hafezi, Moradeshagi, Vaystub & Insel, 1987). There was no evidence, however, that the recovery from an acid load was inhibited by clonidine. The reduction in the magnitude of the acidification, and the fact that pH_i recovered rapidly, suggests that the Na^+–H^+ exchanger was probably stimulated rather than inhibited by clonidine.

Buffering capacity

Since it proved impossible to block the activity of the Na^+–H^+ exchanger pharmacologically, investigation of the HCO_3^- uptake mechanism had to be based upon quantitative comparisons of acid–base fluxes in the presence and absence of HCO_3^- and their sensitivity to H_2DIDS. In order to quantify the net proton fluxes associated with the recovery from an acid load, it was necessary first to measure the buffering capacity of the cytosol since this would be expected to differ significantly in the presence and absence of HCO_3^-. To assess the pH dependence of the cytosolic buffering capacity, we adopted the approach of Weintraub & Machen (1989).

Endpieces were exposed first to a Na^+-free, Hepes-buffered solution (Fig. 6*A*). This caused a marked decrease in pH_i, for reasons that will be discussed below, and it ensured that Na^+-dependent pH regulatory mechanisms did not affect the subsequent events. The endpieces were then stepped through a sequence of Na^+-free solutions containing decreasing concentrations of NH_4Cl. The changes in pH_i associated with the transitions from higher to lower NH_4Cl concentrations were used to calculate the cytosolic β_i. This method makes the assumption that when $[NH_4^+]_o$ is reduced, $[NH_4^+]_i$ decreases through the efflux of NH_3 alone, and the remaining protons acidify the cytosol. By using several different NH_4Cl concentrations, values for β_i were obtained over a range of pH_i values. In case both NH_3 and NH_4^+ were crossing the membrane, the measurements were repeated using the weak base trimethylamine which would be expected to have a less permeant protonated form (Szatkowski & Thomas, 1989). The results of all these measurements are pooled in Fig. 6*B*. Although somewhat scattered, there was little difference between the data obtained with NH_4Cl and trimethylamine. The pooled data were fitted adequately by a sigmoid curve, and the predicted total buffering capacity in the presence of HCO_3^-, β_t, was calculated as described above (see Methods).

Recovery from an acid load in the absence of HCO_3^-

When HCO_3^- is present, the recovery of pH_i following an acid load may occur as a result either of proton extrusion or of HCO_3^- uptake. To evaluate specifically the contribution of Na^+–H^+ exchange, we investigated the effect of acid loading the cells in the absence of HCO_3^-. The results are shown first for unstimulated endpieces (Fig. 7*A*). Removal of Na^+ by substitution with $NMDG^+$ caused a progressive decrease in pH_i towards a steady-state value of approximately 6·5 – as would be predicted if H^+ was approaching electrochemical equilibrium with a membrane potential of approximately −55 mV. When extracellular

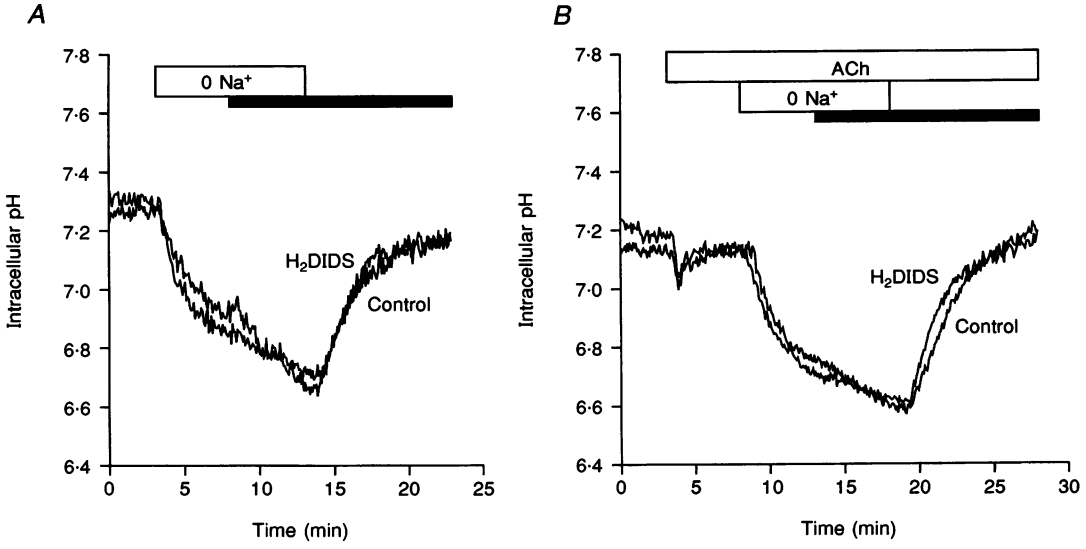

Figure 7. Acid loading by Na^+ substitution in the absence of HCO_3^-

Endpieces were acidified by replacement of Na^+ with $NMDG^+$. *A*, unstimulated endpieces: pH_i changes in cells exposed to 0·5 mM H_2DIDS (filled bar) and in untreated controls. *B*, endpieces stimulated with 1 μM ACh: pH_i changes in cells exposed to H_2DIDS (filled bar) and in untreated controls. Data are representative of at least 5 experiments.

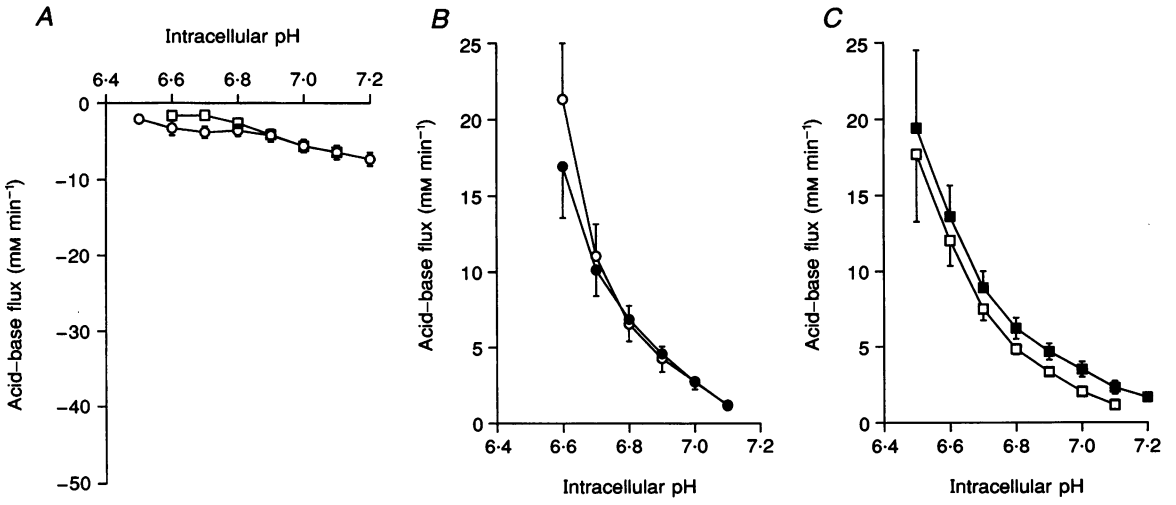

Figure 8. Effects of ACh and H_2DIDS on acid–base fluxes in the absence of HCO_3^-

A, acid loading due to the removal of Na^+ in unstimulated endpieces (○, $n = 16$) and during stimulation with 1 μM ACh (□, $n = 10$). *B*, recovery of pH_i in unstimulated endpieces following restoration of Na^+ in the presence (●, $n = 8$) and absence of 0·5 mM H_2DIDS (○, $n = 8$). *C*, recovery of pH_i in ACh-stimulated endpieces following restoration of Na^+ in the presence (■, $n = 5$) and absence of H_2DIDS (□, $n = 5$). Data were calculated from the changes in pH_i shown in Fig. 7 using the buffering capacity measurements shown in Fig. 6. Positive values represent acid extrusion (or base loading).

Na^+ was restored, pH_i increased rapidly towards its control value, presumably as a result of Na^+–H^+ exchange. When 0·5 mM H_2DIDS was applied during the recovery phase (Fig. 7*A*), pH_i followed a very similar time course, as would be expected in the absence of HCO_3^- uptake mechanisms.

The experiment was then repeated during muscarinic stimulation (Fig. 7*B*). As before, 1 μM ACh caused a small transient decrease in pH_i followed by a partial recovery. Switching to the Na^+-free solution after 5 min of ACh stimulation acidified the cells. The rates of acidification and recovery were similar to those observed in the unstimulated cells, and the recovery phase was not significantly affected by H_2DIDS.

The acid–base fluxes calculated from these changes in pH_i (using the buffering capacity data in Fig. 6) are plotted as a function of pH_i in Fig. 8 where positive values represent

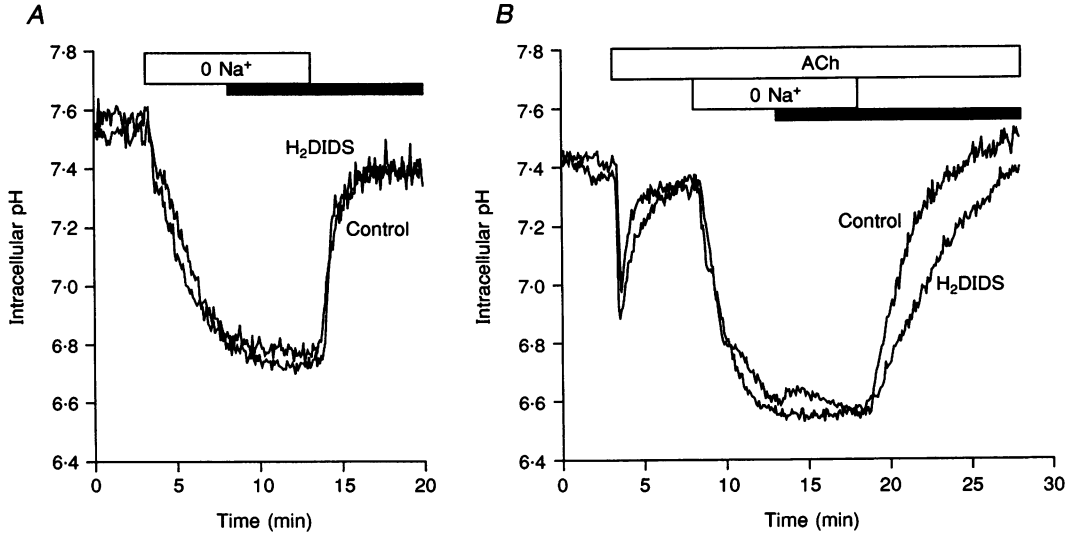

Figure 9. Acid loading by Na^+ substitution in the presence of 25 mM HCO_3^-

Endpieces were acidified by replacement of Na^+ with $NMDG^+$. *A*, unstimulated endpieces: pH_i changes in cells exposed to 0·5 mM H_2DIDS (filled bar) and in untreated controls. *B*, endpieces stimulated with 1 μM ACh: pH_i changes in cells exposed to H_2DIDS (filled bar) and in untreated controls. Data are representative of at least 5 experiments.

acid extrusion (or base loading) and negative values represent acid loading (or base extrusion). The acid loading flux associated with the transition to the Na^+-free solution (Fig. 8*A*) may be due not only to the factors that normally acidify the cells, i.e. H^+ leakage and metabolic acid production, but also to Na^+–H^+ exchange driven by the reversed Na^+ gradient. It is impossible to estimate from these data the relative contributions of these different components. However, the total flux was relatively small compared with that obtained in the presence of HCO_3^- (see below), and it was not significantly affected by ACh stimulation. This suggests that in the absence of HCO_3^-, there was no measurable increase in metabolic acid production or upregulation of the Na^+–H^+ exchanger following stimulation.

The acid extrusion flux responsible for the recovery of pH_i when extracellular Na^+ was restored to the unstimulated cells is shown in Fig. 8*B*. The flux was unaffected by H_2DIDS, was steeply pH dependent and presumably due largely to Na^+–H^+ exchange. The corresponding data obtained from endpieces stimulated with 1 μM ACh (Fig. 8*C*) were virtually identical. This contrasts with the rat mandibular gland in which stimulation causes an alkaline shift of 0·15 pH units as a result of the upregulation of the Na^+–H^+ exchanger (Okada, Saito, Sawada & Nishiyama, 1991; Seo, Larcombe-McDouall, Case & Steward, 1995).

Recovery from an acid load in the presence of HCO_3^-

In the presence of 25 mM HCO_3^-, removal of extracellular Na^+ caused a steeper decrease in pH_i in unstimulated cells (Fig. 9*A*) compared with the equivalent data obtained in the absence of HCO_3^- (Fig. 7*A*). This is despite the greater buffering capacity of the cytosol in the presence of HCO_3^- (Fig. 6*B*) which tends to dampen any change in pH_i. The recovery of pH_i in unstimulated cells when Na^+ was restored was also more rapid than in the absence of HCO_3^-, but was unaffected by H_2DIDS (Fig. 9*A*). In endpieces stimulated with ACh (Fig. 9*B*), the acidification when Na^+ was removed was even more rapid than in the unstimulated cells, whereas the recovery was slower and significantly inhibited by H_2DIDS.

The calculated acid–base fluxes are shown in Fig. 10. The acid loading flux was substantially greater in the presence of HCO_3^-, and was increased even further by ACh stimulation (Fig. 10*A*). Comparison with the much smaller fluxes observed in the absence of HCO_3^- (Fig. 8*A*) suggests that the acid loading flux was due mainly to HCO_3^- efflux either across the luminal membrane or possibly via a Na^+-dependent HCO_3^- uptake mechanism operating in reverse. The acid extrusion flux responsible for the recovery of pH_i was also greater in the presence of HCO_3^- but was not significantly inhibited by H_2DIDS (Fig. 10*B*) suggesting that the Na^+–H^+ exchanger was more active in these cells.

In the ACh-stimulated cells, the recovery of pH_i when Na^+ was restored was slower than in the unstimulated cells, as already noted. This is reflected in the smaller acid extrusion fluxes shown in Fig. 10*C* compared with the fluxes at corresponding pH values in Fig. 10*B*. The reason for this is probably as follows. The acid extrusion flux plotted in Fig. 10*C* (□) is a net flux representing the sum of (i) a relatively large acid extrusion flux due to Na^+-dependent HCO_3^- uptake and Na^+–H^+ exchange, and (ii) a relatively

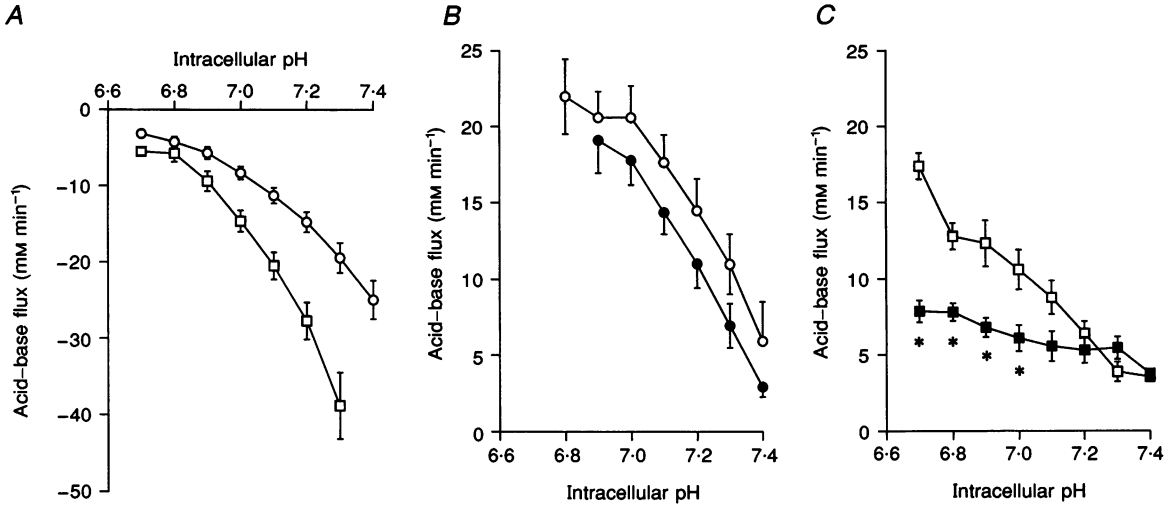

Figure 10. Effects of ACh and H_2DIDS on acid–base fluxes in the presence of 25 mM HCO_3^-

A, acid loading due to the removal of Na^+ in unstimulated endpieces (○, $n = 11$) and during stimulation with 1 μM ACh (□, $n = 12$). *B*, recovery of pH_i in unstimulated endpieces following restoration of Na^+ in the presence (●, $n = 6$) and absence of 0·5 mM H_2DIDS (○, $n = 5$). *C*, recovery of pH_i in ACh-stimulated endpieces following restoration of Na^+ in the presence (■, $n = 6$) and absence of H_2DIDS (□, $n = 6$). Data were calculated from the changes in pH_i shown in Fig. 9 using the buffering capacity measurements shown in Fig. 6. Positive values represent acid extrusion (or base loading).

large acid loading flux due mainly to HCO_3^- efflux. Consequently the net flux plotted in Fig. 10*C* underestimates the magnitude of (i) because of the large negative value of (ii).

Figure 10*C* also shows that during ACh stimulation – in contrast to the unstimulated cells – the net acid extrusion flux was significantly reduced by H_2DIDS. This can only be explained by an inhibition of HCO_3^- uptake and it confirms our earlier conclusion that H_2DIDS has a greater inhibitory effect on HCO_3^- uptake than it does on HCO_3^- efflux. These data therefore provide further support for the hypothesis that a stilbene-sensitive, Na^+-dependent HCO_3^- uptake mechanism exists in the endpiece cells, and that it becomes markedly more active during muscarinic stimulation.

DISCUSSION

Ironically, most of what is known about the efflux of HCO_3^- across the luminal membrane of salivary endpiece cells derives from studies of glands that secrete relatively little HCO_3^-. Transient decreases in pH_i in response to stimulation with ACh have been reported in several glands, and have been attributed to HCO_3^- efflux across the luminal membrane in the rat parotid and rabbit mandibular glands (Nauntofte & Dissing, 1988; Lau *et al.* 1989; Steward *et al.* 1989). In the sheep parotid, we have observed a transient acidification that is similar in time course but somewhat larger in amplitude (approximately 0·4 pH units compared with 0·1–0·2 pH units). Nonetheless, the underlying mechanism resembles that in the rodent glands in the following respects. First, the transient is markedly reduced in amplitude in the absence of HCO_3^- (Fig. 1). Second, the transient is partially blocked by the Cl^- channel blocker NPPB (Fig. 2) and by the stilbene derivative H_2DIDS (Fig. 3). Third, the transient is not significantly diminished when extracellular Cl^- is replaced by gluconate. These results are consistent with our previous data indicating that HCO_3^- crosses the luminal membrane via an anion channel rather than by exchange with Cl^- (Poronnik *et al.* 1995). It is possible that this channel is similar to the non-selective anion channel believed to be responsible for HCO_3^- efflux in the bovine parotid (Lee & Turner, 1992) and in the rabbit mandibular gland (Brown *et al.* 1989).

Analysis of the mechanism of accumulation of intracellular HCO_3^- across the basolateral membrane is more difficult. Intracellular HCO_3^- may be generated either from CO_2 – by the action of carbonic anhydrase combined with basolateral extrusion of H^+ – or by the uptake of HCO_3^- across the basolateral membrane. In the parotid gland of the red kangaroo, *Macropus rufus*, carbonic anhydrase inhibitors largely block secretion of the HCO_3^--rich saliva (Beal, 1991) but in the sheep parotid they have a relatively small effect (Blair-West *et al.* 1980) despite the high activity of the enzyme and the presence of two isoenzymes (Fernley, Wright & Coghlan, 1979). Of the mechanisms that might contribute to H^+ extrusion in the sheep parotid, we can exclude the involvement of a H^+-ATPase for the following reason. In the absence of extracellular Na^+, pH_i approaches electrochemical equilibrium, both in the unstimulated endpiece cells (Fig. 7) and during stimulation with ACh (Fig. 9). This indicates that the mechanism that maintains pH_i and $[HCO_3^-]_i$ above equilibrium is Na^+ dependent. Possible candidates therefore include Na^+–H^+ exchange, Na^+–HCO_3^- cotransport and/or other Na^+-coupled acid or base transporters.

Unfortunately, without an effective inhibitor for the Na^+–H^+ exchanger in the sheep parotid (Poronnik *et al.* 1993), it is difficult to estimate directly the contribution of the exchanger to HCO_3^- accumulation. Furthermore, the only effective inhibitor that we have at present for the Na^+–HCO_3^- cotransporter, H_2DIDS, appears also to block, partially, HCO_3^- efflux across the luminal membrane. In pH experiments this tends to obscure the inhibitory effect of H_2DIDS on the cotransporter. Nonetheless the results presented here suggest that the Na^+–HCO_3^- cotransporter contributes rather more than Na^+–H^+ exchange to the accumulation of intracellular HCO_3^- during ACh stimulation. This is not a unique case – such a mechanism has also been proposed for HCO_3^- secretion in the amphibian gastric mucosa (Curci, Debellis, Caroppo & Frömter, 1994).

In a previous paper (Poronnik *et al.* 1995), we presented measurements of intracellular Na^+ concentration indicating that there is a component of Na^+ uptake across the basolateral membrane which is dependent on HCO_3^-, inhibited by H_2DIDS, independent of Cl^- and stimulated by ACh. Conversely, in the present study, we have shown that there is a component of HCO_3^- uptake during ACh stimulation (and also following acid loading) which is Na^+ dependent and inhibited by H_2DIDS. Our previous study suggested that at least 50% of the increase in $[Na^+]_i$ stimulated by ACh was blocked by a direct action of H_2DIDS on a basolateral Na^+–HCO_3^- cotransporter. To this we can now add the following additional evidence for a significant contribution by Na^+–HCO_3^- cotransport to HCO_3^- uptake during sustained ACh stimulation.

First, the Na^+–H^+ exchanger in the sheep parotid does not appear to be upregulated by ACh stimulation (Fig. 8). This contrasts with other mammalian salivary glands in which a shift in the pH activation curve of the exchanger enables it to maintain H^+ extrusion at elevated values of pH_i (Manganel & Turner, 1989; Steward *et al.* 1989; Okada *et al.* 1991; Seo *et al.* 1995). From this we conclude that, in the sheep parotid, where pH_i rises above the resting level during sustained stimulation, the Na^+–H^+ exchanger is unlikely to be any more active than in the resting condition and may indeed be less active. H^+ extrusion via the exchanger is therefore unlikely to be responsible for much of the accumulation of intracellular HCO_3^- which occurs during ACh stimulation.

Second, in the presence of HCO_3^-, the recovery from an acid load during stimulation with ACh is significantly inhibited by H_2DIDS (Fig. 10). The full extent of this inhibition may however be partially obscured by the inhibitory effect of H_2DIDS on luminal HCO_3^- efflux (Fig. 3) which will tend to have the opposite effect of accelerating the recovery from acidification. Despite this, the recovery from the initial acidification evoked by ACh was inhibited by 66% when H_2DIDS was applied simultaneously with ACh (Fig. 4). This result shows that H_2DIDS has a greater inhibitory effect on HCO_3^- uptake than it does on HCO_3^- efflux. It also provides a lower-limit estimate of the relative contribution of stilbene-sensitive HCO_3^- uptake to the supply of intracellular HCO_3^- for secretion.

Third, H_2DIDS causes a decrease in steady-state pH_i during continuous stimulation with ACh (Fig. 3). This occurs despite the inhibitory effect of H_2DIDS on HCO_3^- efflux, which would otherwise tend to raise pH_i. Assuming that only the Na^+–H^+ exchanger remains active in the presence of H_2DIDS, pH_i would be expected to attain a steady-state value at which the secretory efflux of HCO_3^- is balanced by H^+ extrusion via the exchanger. Our results show that pH_i has to decrease – thus both stimulating the exchanger and reducing the driving force for HCO_3^- efflux – for such a balance to be achieved. Under normal conditions, when pH_i is elevated, the exchanger will be less active and the driving force for HCO_3^-efflux will be greater. It follows, therefore, that Na^+–H^+ exchange will only contribute a fraction of the secreted HCO_3^- and the rest must derive from HCO_3^- uptake, most probably via a stilbene-sensitive Na^+–HCO_3^- cotransporter.

In conclusion, we have shown that there are similarities between the sheep parotid gland and other mammalian salivary glands in the mechanism by which HCO_3^- leaves the cell across the luminal membrane. The mechanism for HCO_3^- uptake across the basolateral membrane differs among species however. In glands that secrete a Cl^--rich primary fluid containing relatively little HCO_3^-, such as the rat and rabbit mandibular glands, the flux of HCO_3^- appears to derive mainly from the action of carbonic anhydrase on CO_2 combined with H^+ extrusion across the basolateral membrane by Na^+–H^+ exchange (Case, Hunter, Novak & Young, 1984; Novak & Young, 1986). Thus, under conditions where Cl^- secretion is abolished, secretion of the remaining HCO_3^--rich fluid is blocked by carbonic anhydrase inhibitors and by amiloride. Some of the ruminant glands that secrete a HCO_3^--rich primary fluid, such as the kangaroo parotid, appear to use the same mechanism and show the same sensitivity to carbonic anhydrase inhibitors and amiloride (Beal, 1991, 1995). In contrast, HCO_3^- secretion by the sheep parotid gland is only partially inhibited by carbonic anhydrase inhibitors (Blair-West *et al.* 1980) and is unaffected by amiloride (Wright *et al.* 1986). Our results indicate that these anomalies are due to a fundamental difference in the basolateral transport mechanism. In the sheep parotid gland, a Na^+–HCO_3^- cotransporter, rather than the Na^+–H^+ exchanger, appears to be responsible for much of the uptake of HCO_3^- during cholinergic stimulation.

Beal, A. M. (1984). Electrolyte composition of parotid saliva from sodium-replete red kangaroos (*Macropus rufus*). *Journal of Experimental Biology* **111**, 225–237.

Beal, A. M. (1991). The effect of carbonic anhydrase inhibitors on secretion by the parotid and mandibular glands of red kangaroos *Macropus rufus*. *Journal of Comparative Physiology* B **161**, 611–619.

Beal, A. M. (1995). Mechanisms of fluid and ion secretion by the parotid gland of the kangaroo, *Macropus rufus*, assessed by administration of transport-inhibiting drugs. *Journal of Comparative Physiology* B **165**, 396–405.

Blair-West, J. R., Fernley, R. T., Nelson, J. F., Wintour, E. M. & Wright, R. D. (1980). The effect of carbonic anhydrase inhibitors on the anionic composition of sheep's parotid saliva. *Journal of Physiology* **299**, 29–44.

Brown, P. D., Elliott, A. C. & Lau, K. R. (1989). Indirect evidence for the presence of non-specific anion channels in rabbit mandibular salivary gland acinar cells. *Journal of Physiology* **414**, 415–431.

Case, R. M. & Argent, B. E. (1993). Pancreatic duct cell secretion: control and mechanisms of transport. In *The Pancreas: Biology, Pathobiology and Disease*, ed. Go, V. L. W., DiMagno, E. P., Gardner, J. D., Lebenthal, E., Reber, H. A. & Scheele, G. A., 2nd edn, pp. 301–350. Raven Press, New York.

Case, R. M., Hunter, M., Novak, I. & Young, J. A. (1984). The anionic basis of fluid secretion by the rabbit mandibular salivary gland. *Journal of Physiology* **349**, 619–630.

Coats, D. A. & Wright, R. D. (1957). Secretion by the parotid gland of the sheep: the relationship between salivary flow and composition. *Journal of Physiology* **135**, 611–622.

Compton, J. S., Nelson, J., Wright, R. D. & Young, J. A. (1980). A micropuncture investigation of electrolyte transport in the parotid glands of sodium-replete and sodium-depleted sheep. *Journal of Physiology* **309**, 429–446.

Cook, D. I. (1995). Salivary secretion in ruminants. In *Ruminant Physiology: Digestion, Metabolism, Growth and Reproduction*, pp. 151–168. Ferdinand Enke Verlag.

Cook, D. I., Van Lennep, E. W., Roberts, M. L. & Young, J. A. (1994). Secretion by the major salivary glands. In *Physiology of the Gastrointestinal Tract*, 3rd edn, vol. 2, ed. Johnson, L. R., pp. 1061–1117. Raven Press, New York.

Curci, S., Debellis, L., Caroppo, R. & Frömter, E. (1994). Model of bicarbonate secretion by resting frog stomach fundus mucosa. I. Transepithelial measurements. *Pflügers Archiv* **428**, 648–654.

Fernley, R. T., Wright, R. D. & Coghlan, J. P. (1979). A novel carbonic anhydrase from the ovine parotid gland. *FEBS Letters* **105**, 299–302.

Gray, M. A., Greenwell, J. R. & Argent, B. E. (1988). Secretin-regulated chloride channel on the apical plasma membrane of pancreatic duct cells. *Journal of Membrane Biology* **105**, 131–142.

Hoppe, P., Kay, R. N. B. & Maloiy, G. M. O. (1975). Salivary secretion in the camel. *Journal of Physiology* **244**, 32–33*P*.

KULANTHAIVEL, P., FURESZ, T. C., MOE, A. J., SMITH, C. H., MAHESH, V. B., LEIBACH, F. H. & GANAPATHY, V. (1992). Human placental syncytiotrophoblast expresses two pharmacologically distinguishable types of Na^+-H^+ exchangers, NHE-1 in the maternal-facing (brush border) membrane and NHE-2 in the fetal-facing (basal) membrane. *Biochemical Journal* **284**, 33–38.

LAU, K. R., ELLIOTT, A. C. & BROWN, P. D. (1989). Acetylcholine-induced intracellular acidosis in rabbit salivary gland acinar cells. *American Journal of Physiology* **256**, C288–295.

LEE, S. I. & TURNER, R. J. (1991). Mechanism of secretagogue-induced HCO_3^- and Cl^- loss from rat parotid acini. *American Journal of Physiology* **261**, G111–118.

LEE, S. I. & TURNER, R. J. (1992). Secretagogue-induced $^{86}Rb^+$ efflux from bovine parotid is HCO_3^- dependent. *American Journal of Physiology* **264**, R162–168.

LEPKE, S., FASOLD, H., PRING, M. & PASSOW, H. (1976). A study of the relationship between inhibition of anion exchange and binding to the red blood cell membrane of 4,4′-diisothiocyano stilbene-2,2′-disulfonic acid (DIDS) and its dihydro derivative (H_2DIDS). *Journal of Membrane Biology* **29**, 147–177.

MANGANEL, M. & TURNER, R. J. (1989). Agonist-induced activation of Na^+/H^+ exchange in rat parotid acinar cells. *Journal of Membrane Biology* **111**, 191–198.

MELVIN, J. E., MORAN, A. & TURNER, R. J. (1988). The role of HCO_3^- and Na^+/H^+ exchange in the response of rat parotid acinar cells to muscarinic stimulation. *Journal of Biological Chemistry* **263**, 19564–19569.

NAUNTOFTE, B. & DISSING, S. (1988). Cholinergic-induced electrolyte transport in rat parotid acini. *Comparative Biochemistry and Physiology* A **90**, 739–746.

NORD, E. P., HOWARD, M. J., HAFEZI, A., MORADESHAGI, P., VAYSTUB, S. & INSEL, P. A. (1987). Alpha$_2$ adrenergic agonists stimulate Na^+-H^+ antiport activity in the rabbit renal proximal tubule. *Journal of Clinical Investigation* **80**, 1755–1762.

NOVAK, I. & GREGER, R. (1988). Properties of the luminal membrane of isolated perfused rat pancreatic ducts. Effects of cyclic AMP and blockers of chloride transport. *Pflügers Archiv* **411**, 546–553.

NOVAK, I. & YOUNG, J. A. (1986). Two independent anion transport systems in rabbit mandibular salivary glands. *Pflügers Archiv* **407**, 649–656.

OKADA, M., SAITO, Y., SAWADA, E. & NISHIYAMA, A. (1991). Microfluorometric imaging study of the mechanism of activation of the Na^+/H^+ antiport by muscarinic agonist in rat mandibular acinar cells. *Pflügers Archiv* **419**, 338–348.

PORONNIK, P., SCHUMANN, S. Y. & COOK, D. I. (1995). HCO_3^- dependent ACh activated Na^+ influx in sheep parotid secretory endpieces. *Pflügers Archiv* **429**, 852–858.

PORONNIK, P., YOUNG, J. A. & COOK, D. I. (1993). Na^+-H^+ exchange in sheep parotid endpieces. Apparent insensitivity to amiloride. *FEBS Letters* **315**, 307–312.

SEO, J. T., LARCOMBE-MCDOUALL, J. B., CASE, R. M. & STEWARD, M. C. (1995). Modulation of Na^+–H^+ exchange by altered cell volume in perfused rat mandibular salivary gland. *Journal of Physiology* **487**, 185–195.

STEWARD, M. C., SEO, Y. & CASE, R. M. (1989). Intracellular pH during secretion in the perfused rabbit mandibular salivary gland measured by ^{31}P NMR spectroscopy. *Pflügers Archiv* **414**, 200–207.

SZATKOWSKI, M. S. & THOMAS, R. C. (1989). The intrinsic intracellular H^+ buffering power of snail neurones. *Journal of Physiology* **409**, 89–101.

THOMAS, J. A., BUCHSBAUM, R. N., ZIMNIAK, A. & RACKER, E. (1979). Intracellular pH measurements in Ehrlich ascites tumor cells utilizing spectroscopic probes generated in situ. *Biochemistry* **18**, 2210–2218.

WEINTRAUB, W. H. & MACHEN, T. E. (1989). pH regulation in hepatoma cells: roles for Na–H exchange, Cl–HCO_3 exchange, and Na–HCO_3 cotransport. *American Journal of Physiology* **257**, G317–327.

WRIGHT, R. D., BLAIR-WEST, J. R. & NELSON, J. F. (1986). Effects of ouabain, amiloride, monensin, and other agents on ovine parotid secretion. *American Journal of Physiology* **250**, F503–510.

YOUNG, J. A. & VAN LENNEP, E. W. (1979). Transport in salivary and salt glands. In *Membrane Transport in Biology*, ed. GIEBISCH, G., TOSTESON, D. C. & USSING, H. H., vol. IVB, pp. 563–674. Springer Verlag, Berlin.

Acknowledgements

This project was supported by the Australian Research Council. M.C.S. was supported by grants from the Royal Society, the Wain Fund of the Agricultural and Fisheries Research Council, and the Dale Fund of The Physiological Society. We thank Professor J. A. Young for his support and encouragement, and Dr Nick Sangster and Mr Roger Murphy for access to their sheep.

Author's email address

M. C. Steward: m.c.steward@man.ac.uk

Received 23 February 1996; accepted 2 April 1996.